



1 The relative importance of antecedent soil moisture and precipitation
2 in flood generation in the middle and lower Yangtze River basin

3

4 Sheng Ye¹, Jin Wang¹, Qihua Ran^{2*}, Xiuxiu Chen¹, Lin Liu¹

5

6 ¹ Institute of Hydrology and Water Resources, School of Civil Engineering, Zhejiang

7 University, Hangzhou 310058, China

8 ² State Key Laboratory of Hydrology-Water Resources and Hydraulic Engineering,

9 Hohai University, Nanjing 210098, China

10

11 * Corresponding author: Qihua Ran

12

13 Email address of the corresponding author: ranqihua@zju.edu.cn

14

15

16

17

18



19 **Abstract**

20 Floods have caused severe environmental and social economic losses worldwide in
21 human history, and are projected to exacerbate due to climate change. Many floods are
22 caused by heavy rainfall with highly saturated soil, however, the relative importance of
23 rainfall and antecedent soil moisture and how it changes from place to place has not
24 been fully understood. Here we examined annual floods from more than 200
25 hydrological stations in the middle and lower Yangtze River basin. Our results indicate
26 that the dominant factor of flood generation shifts from rainfall to antecedent soil
27 moisture with the increase of watershed area. The ratio of the relative importance of
28 antecedent soil moisture and daily rainfall (SPR) is positively correlated with
29 topographic wetness index and has a negative correlation with the magnitude of annual
30 floods. This linkage between watershed characteristics that are easy to measure and the
31 dominant flood generation mechanism provides a quantitative method for flood control
32 and early warnings in ungauged watersheds in the middle and lower Yangtze River
33 basin.

34 **Key words:** flood generation, scaling effect, topographic wetness index

35

36



37 **1. Introduction**

38 Flooding is one of the most destructive and costly natural hazards in the world, resulting
39 in considerable fatalities and property losses (Suresh et al., 2013). River floods have
40 affected nearly 2.5 billion people between 1994 and 2013 worldwide (CRED, 2015),
41 and caused 104 billion dollars losses every year (Desai et al 2015). The damages may
42 be further exacerbated by increasing frequency of extreme rainfall events according to
43 climate change projection (IPCC 2012; Ohmura and Wild 2002). Flood control
44 infrastructures and more accurate predictions are needed to reduce flood damages,
45 which requires better understanding of the underlying mechanism of flood generation.

46 Numerous studies have been conducted to investigate the cause of floods across
47 the world (Bloschl et al 2013; Munoz et al 2018; Zhang et al 2018). Many studies
48 focused on examining the environmental and social characteristics that lead to specific
49 catastrophic flood events (Bloschl et al 2013; Liu et al 2020; Zhang et al., 2018). Others
50 concentrated on single locations, usually catchment outlets, to explore the influential
51 factors of floods and the future trends (Brunner et al., 2016; Munoz et al 2018). Yet
52 given the amount of data and time required, it is not practical to apply these detailed
53 studies to hundreds of catchments to generate an overview of the flood generation
54 mechanism at large scale.

55 Recently, researchers started to investigate the dominant flood generation
56 mechanisms at regional scales (Berghuijs et al 2019b; Do et al 2020; Garg & Mishra
57 2019; Smith et al 2018; Trambly et al 2021; Ye et al 2017). Most of these studies are
58 conducted in North America and Europe with well-documented long-term records
59 (Berghuijs et al 2016; Bloschl et al 2019; Do et al 2020; Musselman et al 2018; Rottler
60 et al 2020). Little work has been conducted on the flood generation mechanisms in



61 China (except Yang et al 2019).

62 As the largest river in China, Yangtze River basin has long suffered from floods. In
63 summer 2020, 378 tributaries of the Yangtze River had floods exceeding the alarm level,
64 causing billions of dollars damage (Xia et al., 2021). With the increasing public
65 awareness, more accurate prediction is needed, which relies on better understanding.
66 However, due to the limitation of observations, there are only a few regional studies of
67 the flood generation mechanism in China, even little in the Yangtze River basin (Zhang
68 et al 2018; Yang et al 2019; Yang et al 2020). The large number of dams and reservoirs
69 built along the river further complicated the situation (Feng et al., 2017; Qian et al 2011;
70 Yang et al 2019).

71 Because of the relatively warm temperature, snowmelt has little impact on flood
72 generation in the Yangtze River basin (Yang et al 2020). Floods in the Yangtze River
73 basin usually occur during summer with relatively wet soil and high rainfall (Wang et
74 al 2021). Heavy rainfall with high antecedent soil moisture has also been identified as
75 dominant driver of floods across world (Beighuijs et al 2019b; Garg et al 2019;
76 Trambly et al 2021; Wasko et al 2020). However, little study examines the relative
77 importance of rainfall and antecedent soil moisture in flood generation. A quantitative
78 overview of how the combination of rainfall and antecedent soil moisture change across
79 watersheds is currently unavailable in China (Liu et al., 2021; Wu et al., 2015).

80 Based on the watersheds in the middle and lower Yangtze River basin, this study
81 attempts to explore the following questions: 1) is there a way to quantitatively describe
82 the relative importance of antecedent soil moisture and rainfall on flood generation; and
83 2) how would this combination of flood-generation rainfall and soil moisture vary
84 across watersheds, and what are the influential factors. Based on the observations and



85 model estimation (Section 2), the spatial distribution patterns of antecedent soil
86 moisture and rainfall were obtained and analyzed to investigate their individual
87 contribution to flood generation and the influential factors (Section3). This allows for
88 further examination of the relative importance of antecedent soil moisture and rainfall
89 on flood generation and its linkage to watershed characteristics as well as its
90 implications to flood prediction (Section 4), all the results are summarized in Section 5.

91 **2 Methods**

92 **2.1 Study area**

93 Yangtze River is the largest river in China, with a total length of 6,300 kilometers and
94 annual discharge of 920km³ at the outlet (Yang et al., 2018). It drains through an area
95 of 1.8*10⁶ km², lying between 90°33'and 122°25'E and 24°30'and 35°45'N, and is
96 home to over 400 million people, most of which live in the middle and lower Yangtze
97 River basin (YZRB) (Cai et al., 2020). The elevation of the YZRB declines from west
98 to east: from over 3000m in Qinghai-Tibet Plateau, to around 1000m in the central
99 mountain region, and the 100m in Eastern China Plain (Wang et al., 2013). The
100 vegetation types in the YZRB are forests, shrubs, grassland and agricultural land,
101 accounting for 11.85%, 12.65%, 32.26% and 42.88% respectively. Grassland and
102 shrubs are the dominant vegetation in the middle and upper YZRB, while the
103 downstream YZRB is dominated by forests and agricultural land (Miao et al., 2010).
104 There are more than 51,000 reservoirs of different sizes in the whole basin, including
105 280 large ones (Peng et al., 2020).

106 Most of the YZRB is semi-humid and humid, with s a typical subtropical monsoon
107 climate. The mean annual temperature is approximately 13.0 °C, varying from -4 °C



108 to 18°C downstream. The mean annual precipitation of the whole basin is about 1200
109 mm, increasing from 300mm in the western headwaters to 2400 mm downstream. (Li
110 et al., 2021). Most of the precipitation comes between June and September, the premise
111 of persistent heavy rain in the Yangtze River basin is the frequent activity of weak cold
112 air in the north (Tao et al., 1980) and the intersection of mid-latitude air mass and
113 monsoon air mass (Kato et al., 1985). Studies have found that both annual precipitation
114 and the frequency of extreme precipitation events have increased in the middle and
115 lower reaches of the Yangtze River (Qian et al., 2020; Fu et al., 2013). As a result, floods
116 have occurred frequently in the middle and lower reaches of the Yangtze River, where
117 most of the population in the YZRB live (Liu et al., 2018).

118 2.2 Data

119 In this work, we focus on the middle and lower reaches of the Yangtze River for the
120 high population density and increasing flood risk. The 30-meter digital elevation model
121 (DEM) was downloaded from Geospatial Data Cloud (<http://www.gscloud.cn/>), from
122 which the drainage area corresponding to the hydrological station was extracted by
123 ArcGIS. Daily precipitation data and temperature data between 1970 and 2016 from
124 247 meteorological stations within and near the YZRB were downloaded from China
125 Meteorological Data Network (<https://data.cma.cn/>). The temperature data was used to
126 estimate potential evaporation. The observed precipitation and estimated potential
127 evaporation were interpolated into the whole YZRB using Thiessen polygon method
128 (Meena et al., 2013). The interpolated precipitation and potential evaporation were then
129 averaged for the drainage area corresponding to each hydrological station.

130 The daily streamflow data was collected from 267 stations from Annual
131 Hydrological Report of the People's Republic of China. Among which, 224 stations



132 with at least 20 years records from 1970 to 1990 and from 2007 to 2016 were selected.
133 Information of 361 reservoirs in the middle and lower YZRB, including capacity and
134 controlling area was downloaded and extracted from the Global Reservoir and Dam
135 database (GRanD) (Lehner et al 2011). Previous study showed that this database
136 provides reliable information of middle and large reservoirs in China (Yang et al 2021).
137 Watersheds with more than 80% of the drainage area under control reservoirs according
138 to GRanD database and/or located right downstream of reservoirs and water gates were
139 considered as watersheds under strong regulation (regulated watersheds).

140 2.3 Calculation of hydrological and topographic characteristics

141 *Potential evaporation estimation*

142 The temperature data was used to estimate potential evaporation following the
143 Hargreaves method (Allen et al., 1998; Vicente et al., 2014; Berti et al., 2014).

$$144 \quad ET_0 = 0.0023 \times (Tmax - Tmin)^{0.5} \times (Tmean + 17.8) \times Ra \quad (1)$$

145 where ET_0 is potential evaporation (mm/d), $Tmax$ is the highest temperature (°C), $Tmin$
146 is the lowest temperature (°C), $Tmean$ is the mean temperature (°C), and Ra is the outer
147 space radiation [$MJ/(m^2 d)$], which can be calculated as follows:

$$148 \quad Ra = 37.6 \times d_r \times (\omega_s \sin \varphi \sin \delta + \cos \varphi \sin \delta \sin \omega_s), \quad (2)$$

149 where d_r is the reciprocal of the relative distance between the sun and the earth, ω_s is
150 the angle of sunshine hours, δ is the inclination of the sun (rad), φ is geographic
151 latitude (rad). d_r , δ and ω_s can be calculated by the following formula:

$$152 \quad d_r = 1 + 0.033 \times \cos\left(\frac{2\pi J}{365}\right), \quad (3)$$



$$153 \quad \delta = 0.409 \times \sin\left(\frac{2\pi J}{365} - 1.39\right), \quad (4)$$

$$154 \quad \omega_S = \arccos(-\tan \varphi \tan \delta), \quad (5)$$

155 where J is the daily ordinal number (January 1st is 1).

156 *Soil water storage estimation*

157 The soil water storage was estimated based on the daily water balance (Berhuijs et al.,
158 2019; Deb et al., 2019):

$$159 \quad \frac{dS}{dt} = P - ET - \max(Q, 0), \quad (6)$$

160 Where S is the soil water storage (mm); P is precipitation (mm/d), Q is discharge
161 normalized by area (mm/d), ET is evaporation (mm/d), which can be calculated from
162 potential evapotranspiration (ET_0):

$$163 \quad ET = \min(0.75 \times ET_0, S), \quad (7)$$

164 *Topographic wetness index estimation*

165 Topographic wetness index was calculated to represent the combined impacts of
166 drainage area and topographic gradient (Alfonso et al., 2011; Grabs et al., 2009):

$$167 \quad TWI = \ln(A_d / \tan \alpha), \quad (8)$$

168 where A_d is drainage area and α is topographic gradient estimated from DEM.

169 **2.4 Quantification of the relative importance of soil moisture and precipitation** 170 **during floods**

171 The maximum discharge of each year was selected as annual flood, which was then



172 averaged across years as the mean annual maximum flood (AMF). The observed
173 rainfall on that day and the estimated soil water storage at the day before were also
174 averaged across years as daily rainfall (P) and antecedent soil moisture (S_0). To examine
175 the impacts from long-lasting rainfall event, we also calculated the mean accumulated
176 rainfall from two days (rainfall on the flood day and the day before, P_2) to seven days
177 (weekly rainfall, P_7).

178 The antecedent soil moisture (S_0) was normalized by the maximum soil moisture
179 (S_{max}) to approximate the saturation rate (S') as a surrogate of the contribution of soil
180 moisture in flood generation. The daily rainfall (P) was normalized by the maximum
181 daily rainfall (P_{max}) to show the relative intensity (P'), representing the contribution
182 of rainfall in flood generation. The accumulated rainfall was also normalized by the
183 maximum two-day to seven-day rainfall.

184 To quantify the relative importance of antecedent soil moisture and rainfall in flood
185 generation, the ratio between these two factors at the AMFs was derived: $SPR = S'/P'$.
186 When SPR is larger than 1, floods at those sites are more dominated by antecedent soil
187 moisture; when SPR is less than 1, rainfall is the primary driver of floods.

188 **3 Results**

189 **3.1 Spatial patterns of antecedent soil moisture and precipitation during floods**

190 Because of the latitude and the relative warm climate, floods in the middle and lower
191 Yangtze River basin usually occur in summer, with little influence of snowmelt (Wang
192 et al., 2015; Yang et al 2019). Therefore, in this study we mainly focus on the impacts
193 of antecedent soil moisture and rainfall on flood generation. Figure 2 shows the spatial
194 distribution of normalized antecedent soil moisture and daily rainfall during the annual



195 maximum floods (AMF) in the middle and lower reaches of the Yangtze River.

196 As we can see from Figure 2a, in the middle and lower reaches of YZRB, when
197 AMFs occurred, the antecedent soil saturation rate was generally higher at sites along
198 the major tributaries (i.e., >0.6): the farther away from the main stream, the more
199 saturated the soil was. On the other hand, along and near the main stream and the delta,
200 the antecedent soil saturation rate could be less than 0.4. This may be attributed to the
201 more complicated flood generation mechanism at large scale as well as the strong
202 reservoir control on main stream and water gates regulation in the delta (Gao et al.,
203 2018; Long et al., 2020; Zhang et al., 2017).

204 Figure 2b shows the normalized daily rainfall during the AMFs. As we can see,
205 the daily rainfall is relatively high (>0.4) at more than half of the study sites, while it is
206 small (<0.2) for the sites along the main stream, main tributaries, and in the delta
207 (Figure 2b). Comparison between Figure 2a and b suggests that, except the sites on the
208 main stream and in the delta, sites with relatively high antecedent soil saturation rate
209 (i.e., >0.8 , the green dots) during AMFs are also the ones with relatively small daily
210 rainfall contribution (i.e., <0.2 , the red dots). That is, for these sites, the AMFs are
211 usually occurring at a near saturated soil condition while heavy rainfall at flood day is
212 not necessary, suggesting the relative importance of soil saturation rate. For the sites
213 with both saturation rate and normalized rainfall between 0.4 and 0.6, both the
214 antecedent soil saturation and rainfall play important roles in flood generation. As for
215 the sites on the main stream and in the delta, both antecedent soil moisture and rainfall
216 are low during AMFs, this is likely due to the regulations from large reservoirs and
217 water gates.

218 **3.2 The scaling effect in the contribution of antecedent soil moisture and rainfall**



219 To further investigate the contribution of antecedent soil moisture and rainfall in flood
220 generation and the potential influential factors, we examined their correlation with
221 catchment area (Figure 3). Given the complicated environmental and social impacts,
222 the regulated watersheds and sites on the main stream are presented separately (the
223 green dots and red dots in Figure 3 respectively). Our study will focus on the sites that
224 are not dominated by regulation (the blue dots in Figure 3), for simplicity, we will refer
225 them as natural watersheds.

226 As we can see from Figure 3, during the occurrence of AMFs, the antecedent soil
227 saturation rate increase with watershed area (p -value<0.001), while the normalized
228 daily rainfall decreases with watershed area (p -value<0.001). That is, with the increase
229 of watershed size, antecedent soil moisture becomes more and more important in flood
230 generation while the contribution of daily rainfall declines. On the other hand, heavy
231 rainfall in a single day could only be the dominant driver of floods when watershed area
232 is smaller than 1000km².

233 As for the regulated watersheds (green dots in Figure 3), there is no clear
234 correlation between drainage area and antecedent soil saturation rate or normalized
235 rainfall, which is understandable. Meanwhile, both antecedent soil saturation rate and
236 normalized rainfall decreases with watershed area for main stream sites. One
237 explanation is flood regulation: as the major responsibilities of reservoirs on the main
238 stream are to reduce peak flow and postpone the time to flood peak (Volpi et al., 2018).
239 The other explanation is that when watershed size is larger than 100,000km², the impact
240 of antecedent soil moisture declines. To examine this hypothesis, more data from
241 watersheds larger than 100,000km² and with limited human intervention is needed.
242 However, this is above the scope of this work and requires future studies.



243 3.3 The scaling impacts on accumulated rainfall

244 The saturation of soil before floods could be due to previous rainfall events, and could
245 also be caused by accumulated rainfall in long-lasting rainfall events that eventually
246 generate floods (Xie et al., 2018). Figure 4 presents the correlation between normalized
247 accumulated rainfall and drainage area. When single day rainfall is considered, it is
248 negatively correlated with drainage area (Figure 3a); when accumulated rainfall is
249 considered, the correlation gradually shifts from negative to positive correlation (Figure
250 4). For example, when two-day rainfall was examined, the correlation between
251 accumulated rainfall and drainage area shifts from negative to positive at 1000 km²; the
252 negative correlation in Figure 3a is only valid for watersheds larger than 1000 km²
253 (Figure 4a). This transition area increases from 1000 km² for two-day rainfall to 10,000
254 km² for three-day rainfall (Figure 4b), and 100,000 km² for five-day rainfall (Figure
255 4c). Eventually, the weekly rainfall has similar positive correlation with drainage area
256 like antecedent soil moisture (Figure 4f). The increase of transition area may be
257 explained by the increasing response time and confluence time in large watersheds: it
258 takes days for the flow events generated by heavy rainfall to reach outlets where it can
259 be observed in large watersheds. This is also consistent with the conclusion in the
260 Yellow River Basin (Ran et al., 2020) and our previous findings of the dominant flood
261 generation mechanism in the middle and lower YZRB: weekly rainfall is the dominant
262 flood driver for sites on the main streams and the major tributaries (Wang et al 2021).
263 The regulated watersheds don't show significant correlation which is understandable
264 for the strong human intervention. For the negative correlation between accumulated
265 rainfall and drainage area at main stream sites, it is difficult to decide whether it is due
266 to scaling effect or human intervention.



267 **3.4 The interlink of watershed characteristics, flood, antecedent soil moisture and**
268 **rainfall**

269 Figure 5 presents the contribution of antecedent soil moisture and rainfall to the AMFs
270 at the study watersheds, the circles are scaled by watershed size and colored with
271 topographic gradient. Except the watersheds with strong human intervention (regulated
272 ones and the ones on main stream), there is a negative correlation between the
273 contribution of rainfall and antecedent soil moisture, indicating the shift of dominance
274 from rainfall to antecedent soil moisture across watersheds.

275 Figure 6 shows the influential factors of the relative importance of antecedent soil
276 moisture and rainfall. For the natural watersheds (the circles), SPR increases with
277 drainage area and declines with topographic gradient. That is, the larger the drainage
278 area is, the more essential the contribution of antecedent soil moisture to floods is, and
279 the less influential rainfall is in flood generation. For watersheds with similar drainage
280 area (i.e., the blue and light blue dots in Figure 6b), topographic gradient also cast
281 impacts on SPR: SPR decreases with slope. That is, the relative importance of rainfall
282 increases at steeper watersheds. This may be attributed to the shortened hydrological
283 response time due to the steep topography which facilitates rainfall induced floods
284 generation. As a combination of both drainage area and topographic gradient, TWI is
285 positively correlated with SPR at natural watersheds, with less scatter than the
286 correlation between SPR and drainage area or topographic gradient alone. There is also
287 positive correlation between SPR and TWI for the regulated watersheds along
288 tributaries (black triangles), though much scatter. However, the sites on main stream
289 show opposite pattern: the SPR at these sites decreases with TWI and drainage area. It
290 is difficult to determine whether this is because of reservoir regulation or not. More data



291 about watersheds larger than 10,000km² but with limited human intervention are
292 needed to examine this hypothesis.

293 Besides TWI, SPR is also correlated with the magnitude of AMF (Figure 7). As
294 Figure 7 shows, the area normalized flood peak declines with flood-generation SPR.
295 Watersheds with large flood peak are mostly the ones with steep topographic gradient
296 and small SPR (i.e., SPR<1) and *vice versa*. Similar correlation was also found at event
297 scale in our experimental mountainous watershed, which locates at a headwater of
298 Yangtze River (Liu et al 2021).

299 **4 Discussion**

300 **4.1 The relative importance of antecedent soil moisture and rainfall in flood** 301 **generation**

302 While soil moisture and rainfall are the two main drivers of floods in the middle and
303 lower Yangtze River basin, the dominance of each factor varies across watersheds.
304 Floods in large watershed are usually generated when soil is almost saturated despite
305 of the relatively small rainfall amount, while heavy rainfall is the dominant driver in
306 small to medium watersheds (Figure 3). This shift of dominance may be attributed to
307 the longer confluence time in the large watersheds and the fact that small watershed is
308 easy to reach saturation (Sharma et al., 2018). The rising contribution of antecedent soil
309 moisture in large watersheds was consistent with the findings in Australian watersheds
310 (Wasko & Nathan, 2019); and the declining influence of rainfall at larger watersheds
311 was also found in Indian watersheds (Garg et al 2019).

312 As a result, the natural watersheds in Figure 5 could be grouped into three classes
313 based on their drainage area and topographic gradient. When a watershed is large and



314 flat, flood occurrence is mainly determined by soil saturation; when a watershed is
315 small and steep, heavy rainfall takes over the dominance; when a watershed is small
316 and the topographic gradient is also gentle, the occurrence of AMF requires both highly
317 saturated soil and relatively heavy rainfall.

318 **4.2 Linkage between topographic characteristics, SPR and floods**

319 The correlation between TWI and SPR (Figure 6c) suggests that the relative importance
320 of soil moisture and rainfall could be inferred from topographic characteristics. Despite
321 of the strong human intervention, this correlation sustains even in those regulated
322 watersheds (black squares in Figure 6c). That is, we could derive the relative dominance
323 of soil moisture and rainfall in flood generation in specific watershed from its TWI.
324 This helps quantify the importance of soil moisture and rainfall in flood generation in
325 the existing work. Rainfall and soil moisture level have been identified as dominant
326 drivers of floods, individually or together, in watersheds worldwide (Berghuijs et al
327 2016, 2019b; Garg & Mishra 2019; Trambly et al 2021; Ye et al 2017). Our findings
328 further identified the influential factors of their importance and provide a way to
329 quantitatively estimate it from topographic characteristics that are easy to measure.

330 Meanwhile, the SPR also present a negative correlation with the magnitude of
331 AMFs (Figure 7). Similar correlation was also found in the observations from our
332 experimental watershed, a headwater of Yangtze River (Liu et al 2021). The ratio of
333 observed antecedent soil moisture and event precipitation also presents similar decline
334 trend with discharge at event scale. That suggests that the negative correlation between
335 flow and SPR is not only valid across watersheds, and may also be applied at event
336 scale within watershed.



337 That is, based on the topographic characteristics, we could derive the relative
338 importance of soil moisture and rainfall in flood generation (SPR); and from this
339 relative importance ratio, we could further infer the average flood magnitude at these
340 watersheds. As a result, we could link the topographic characteristics and annual floods
341 through the characteristic SPR during the AMFs.

342 4.3 Implications

343 These findings could be helpful for potential flood risk evaluation and early warning in
344 ungauged basins, e.g., headwaters in the mountainous region. With the construction of
345 large reservoirs, the capability of flood risk control has improved substantially along
346 main stream (Zou et al., 2011; Zhang et al., 2015). However, it is still difficult for early
347 warnings in upstream mountainous watersheds, which are vulnerable to floods but
348 difficult for hydrological modeling and prediction due to little hydrologic records.

349 Our findings suggest that we could derive the flood-generation SPR of each
350 watershed from drainage area and topographic gradient that are easy to measure. Using
351 the soil moisture from remote sensing data and precipitation forecast, we could have
352 real-time prediction of SPR values. Once the predicted SPR value gets closer to the
353 flood-generation SPR in Figure 6c, early warnings of floods can be generated.
354 Mountainous watersheds are usually small and steep, where heavy rainfall is the
355 dominant driver of AMFs (Figure 5). Thus, the requirement of the accuracy of
356 antecedent soil moisture would be lower, soil moisture from recent remote sensing
357 images may be used for approximation. Combining with real-time precipitation forecast,
358 early warnings of AMFs could be generated once the estimated SPR is close to the
359 flood-generation SPR. Besides, the correlation between SPR and flood peak provides
360 information of the likely flood magnitude in ungauged watersheds. Flood control



361 infrastructures could then be designed based on the potential flood peak derived from
362 the flood-generation SPR that is estimated from topographic characteristics.

363 **4.4 Limitations**

364 Previous works usually identify the dominant flood generation mechanism based on the
365 comparison of the timing of events (Berghuijs et al 2016; 2019b; Bloschl et al 2017; Ye
366 et al 2017). Similar work has been implemented in our study watersheds, suggesting
367 the importance of soil moisture and rainfall (Wang et al 2021). Based on that, we further
368 looked into the records to quantitatively evaluate the relative importance of soil
369 moisture and rainfall in flood generation. However, there are limitations in our methods.

370 The precipitation data we used were averaged for the study watersheds from 247
371 meteorological stations. Given the large area and considerable spatial heterogeneity, the
372 precipitation data we used may not always be representative of the actual precipitation
373 events. The daily data could also average the rainfall intensity at hourly scale, which
374 could be influential in small mountainous watersheds. The estimation of soil moisture
375 is for sure highly simplified, which cannot be considered as precise estimation. Yet,
376 after normalizing by the maximum, this can still provide the generation variation trend
377 of soil moisture in the water cycle, and used for the relative comparison with rainfall.
378 For further implementation of this method, more sophisticated models or remote
379 sensing data are needed to improve our estimation of soil moisture, and refine the
380 estimation of the flood-generation SPR.

381 Moreover, this work is focused on the importance soil moisture and rainfall,
382 without consideration of snowmelt due to the warm and humid climate in the study
383 watersheds. To apply our findings to cold watersheds with significant impact of snow,



384 the snowmelt component needs to be incorporated. In addition, our method is based on
385 the average values from many years. While previous work indicated that the occurrence
386 of floods in our study watersheds are highly concentrated (Wang et al 2021), there could
387 be strong inter-annual variability in other watersheds. In future studies, annual scale
388 and event scale analysis are needed to examine and improve our findings before it can
389 be applied to watersheds with more diverse climate and landscape conditions.

390 **5 Conclusions**

391 Heavy rainfall on highly saturated soil was identified as the dominant flood generation
392 mechanism across world (Berghuijs et al 2019; Wang et al 2021; Wasko et al 2020).
393 This study aims to further evaluate the relative importance of antecedent soil moisture
394 and rainfall on floods generation and the controlling factors. Climate and hydrological
395 data from 224 hydrological stations and 247 meteorological stations in the middle and
396 lower reaches of the Yangtze River basin was analyzed, along with the modeled soil
397 moisture. Except the regulated watersheds, the relative importance of antecedent soil
398 moisture and daily rainfall present significant correlation with drainage area: the larger
399 the watershed is, the more essential antecedent soil saturation rate is in flood generation,
400 the less important daily rainfall is.

401 Using the antecedent soil saturation rate and normalized rainfall as coordinates, the
402 flood generation mechanism(s) of study watersheds could be grouped into three classes:
403 antecedent soil moisture dominated large watersheds, heavy rainfall dominated steep
404 and small to middle size watersheds, and small to middle size watersheds with gentle
405 topographic gradient where floods occurrence requires both highly saturated soil and
406 heavy rainfall. Our analysis further shows that the ratio of relative importance between
407 antecedent soil moisture and rainfall (SPR) can be predicted by topographic wetness



408 index. When the topographic wetness index is large, the dominance of antecedent soil
409 moisture for extreme floods is stronger, and *vice versa*. The SPR also presents negative
410 correlation with area normalized flood peak.

411 With the potential increase of extreme rainfall events (Gao et al., 2016; Chen et
412 al., 2016), upstream mountainous watersheds in the middle and lower Yangtze River
413 basin are facing higher risk of extreme floods. The lack of hydrological records further
414 increases the vulnerability of people in these watersheds. Our findings provide a
415 quantitative way to estimate the possible flood risk for these ungauged watersheds.
416 Based on measurable watershed characteristics (i.e., drainage area and topographic
417 gradient), the flood-generation SPR of each watershed can be derived. The real-time
418 SPR can be approximated by recent soil moisture data from remote sensing images and
419 real-time rainfall forecast, especially in the small and steep watersheds where heavy
420 rainfall is the most dominant factor. Early warnings could then be generated once the
421 real-time SPR approaches the flood-generation SPR. Flood control infrastructures
422 could also be designed based on the flood magnitude estimated from the flood-
423 generation SPR.

424 Future analysis at event scale could help generate the flood-generation curve
425 between SPR and discharge at event scale to further improve flood risk predictions in
426 these small ungauged watersheds. With more data from other regions and improved
427 estimation or observation of soil moisture, we could expand our analysis to watersheds
428 with more diverse climate and topographic characteristics to examine and refine our
429 findings and to enhance our understandings of flood generation.

430

431 **Data availability**



432 DEM data was downloaded from Geospatial Data Cloud at <http://www.gscloud.cn/>.
433 Climatological data used in this study was obtained from China Meteorological Data
434 Network, which can be accessed at <http://data.cma.cn/>. Discharge data comes from
435 Annual Hydrological Report of the People's Republic of China issued by Yangtze River
436 Water Resources Commission.

437

438 **Acknowledgements**

439 This research was funded by the National Key Research and Development Program of
440 China (2019YFC1510701-01), and National Natural Science Foundation of China
441 (51979243).

442

443 **References**

- 444 Abbas, S.A., Xuan, Y. and Song, X.: Quantile Regression Based Methods for
445 Investigating Rainfall Trends Associated with Flooding and Drought Conditions.
446 Water Resources Management, 33(12), 4249-4264, [https://doi:10.1007/s11269-](https://doi:10.1007/s11269-019-02362-0)
447 019-02362-0, 2019.
- 448 Alfonso R., Nilza M. R.C., and Anderson L. R.: Numerical Modelling of the
449 Topographic Wetness Index: An Analysis at Different Scales, International
450 Journal of Geosciences(4), 476-483, <https://doi:10.4236/ijg.2011.24050>, 2011.
- 451 Allen R. G., Pereira L. S. and Raes D.: Crop evapotranspiration-Guidelines for
452 computing crop water requirements FAO Irrigation and drainage paper
453 NO.56(Electric Publication)[M], Rome , Italy:FAO, 1998.
- 454 Berghuijs, W.R., Allen, S.T., Harrigan, S. and Kirchner, J.W.: Growing Spatial Scales
455 of Synchronous River Flooding in Europe. Geophysical Research Letters, 46(3),
456 1423-1428, <https://doi:10.1029/2018GL081883>, 2019a.
- 457 Berghuijs, W.R., Harrigan, S., Molnar, P., Slater, L.J. and Kirchner, J.W.: The Relative
458 Importance of Different Flood-Generating Mechanisms Across Europe. Water
459 Resources Research, 55(6), 4582-4593, <https://doi:10.1029/2019WR024841>,
460 2019b.
- 461 Berghuijs, W.R., Woods, R.A., Hutton, C.J. and Sivapalan, M.: Dominant flood
462 generating mechanisms across the United States. Geophysical Research Letters,
463 43(9), 4382-4390, <https://doi:10.1002/2016GL068070>, 2016.



-
- 464 Blöschl, G., Nester, T., Komma, J., Parajka, J. and Perdigao, R.A.P.: The June 2013
465 flood in the Upper Danube Basin, and comparisons with the 2002, 1954, and 1899
466 floods. *Hydrol. Earth Syst. Sci.*, 17, 5197–5212, 2013.
- 467 Blöschl, G., Hall, J., Parajka, J., Perdigão, R. A., Merz, B., Arheimer, B., et al.:
468 Changing climate shifts timing of European floods. *Science*, 357(6351), 588–
469 590. <https://doi.org/10.1126/science.aan2506>, 2017.
- 470 Blöschl, G., Hall, J., Viglione, A., Perdigao, R.A., Parajka, J., Merz, B., et al.: Changing
471 climate both increases and decreases European river floods, *Nature*, 573, 108 –
472 111, 2019.
- 473 Berti, A., Tardivo, G., Chiaudani, A., Rech, F. and Borin, M.: Assessing reference
474 evapotranspiration by the Hargreaves method in north-eastern Italy. *Agricultural
475 Water Management*, 140, 20-25, <https://doi:10.1016/j.agwat.2014.03.015>, 2014.
- 476 Brunner, M. I., Seibert, J. and Favre, A.C.: Bivariate return periods and their importance
477 for flood peak and volume estimation. *Water*, 3, 819 – 833.
478 <https://doi.org/10.1002/wat2.1173>, 2016.
- 479 Brunner, M. I., Gilleland, E., Wood, A., Swain, D. L., and Clark, M.: Spatial
480 dependence of floods shaped by spatiotemporal variations in meteorological and
481 land - surface processes. *Geophysical Research Letters*, 47, e2020GL088000.
482 <https://doi.org/10.1029/2020GL088000>, 2020.
- 483 Cai, Q. H.: Great protection of Yangtze River and watershed ecology, *Yangtze River
484* (01), 70-74, <https://doi:10.16232/j.cnki.1001-4179.2020.01.011>, 2020.
- 485 Cen, S.-x., Gong, Y.-f., Lai, X. and Peng, L.: The Relationship between the
486 Atmospheric Heating Source/Sink Anomalies of Asian Monsoon and
487 Flood/Drought in the Yangtze River Basin in the Meiyu Period. *Journal of
488 Tropical Meteorology*, 21(4), 352-360, 2015.
- 489 Chen, Y. and Zhai, P.: Mechanisms for concurrent low-latitude circulation anomalies
490 responsible for persistent extreme precipitation in the Yangtze River Valley.



-
- 491 Climate Dynamics,47(3-4), 989-1006, <https://doi.org/10.1007/s00382-015-2885-6>,
492 2016.
- 493 CRED (2015). The human cost of natural disasters: A global perspective: Centre for
494 research on the epidemiology of disasters.
- 495 Deb, P., Kiem, A.S. and Willgoose, G.: Mechanisms influencing non-stationarity in
496 rainfall-runoff relationships in southeast Australia. *Journal of Hydrology*, 571,
497 749-764, <https://doi.org/10.1016/j.jhydrol.2019.02.025>, 2019.
- 498 Desai, B., Maskrey, A., Peduzzi, P., De Bono, A., & Herold, C. Making Development
499 Sustainable: The Future of Disaster Risk Management. Global Assessment Report
500 on Disaster Risk Reduction <http://archive-ouverte.unige.ch/unige:78299> (UNISDR,
501 2015).
- 502 Do, H. X., Mei, Y., & Gronewold, A. D.: To what extent are changes in flood magnitude
503 related to changes in precipitation extremes? *Geophysical Research Letters*, 47,
504 e2020GL088684. <https://doi.org/10.1029/2020GL088684>, 2020.
- 505 Fang, X. and Pomeroy, J.W.: Impact of antecedent conditions on simulations of a flood
506 in a mountain headwater basin. *Hydrological Processes*, 30(16), 2754-2772,
507 <https://doi.org/10.1002/hyp.10910>, 2016.
- 508 Feng, B. F., Dai M. L. and Zhang T.: Effect of Reservoir Group Joint Operation on
509 Flood Control in the Middle and Lower Reaches of Yangtze River, *Journal of*
510 *Water Resources Research* (3), 278-284, <https://doi.org/10.12677/JWRR.2017.63033>,
511 2017.
- 512 Fu, G., Yu, J., Yu, X., Ouyang, R., Zhang, Y., Wang, P., Liu, W. and Min, L.: Temporal
513 variation of extreme rainfall events in China, 1961-2009. *Journal of Hydrology*,
514 487, 48-59, <https://doi.org/10.1016/j.jhydrol.2013.02.021>, 2013.
- 515 Gao, T. and Xie, L.: Spatiotemporal changes in precipitation extremes over Yangtze
516 River basin, China, considering the rainfall shift in the late 1970s. *Global and*
517 *Planetary Change*, 147, 106-124, <https://doi.org/10.1016/j.gloplacha.2016.10.016>,
518 2016.
- 519 Gao, Y., Wang, H., Lu, X., Xu, Y., Zhang, Z. and Schmidt, A.R.: Hydrologic Impact
520 of Urbanization on Catchment and River System Downstream from Taihu Lake.
521 *Journal of Coastal Research*, 82-88, <https://doi.org/10.2112/SI84-012.1>, 2018.



-
- 522 Garg, S., & Mishra, V.: Role of extreme precipitation and initial hydrologic conditions
523 on floods in Godavari river basin, India. *Water Resources Research*, 55, 9191–
524 9210. <https://doi.org/10.1029/2019WR025863>, 2019.
- 525 Grabs, T., Seibert, J., Bishop, K. and Laudon, H.: Modeling spatial patterns of saturated
526 areas: A comparison of the topographic wetness index and a dynamic distributed
527 model. *Journal of Hydrology*, 373(1-2), 15-23,
528 <https://doi:10.1016/j.jhydrol.2009.03.031>, 2009.
- 529 IPCC. *Managing the Risks of Extreme Events and Disasters to Advance Climate*
530 *Change Adaptation* (eds Field, C. B. et al.) (Cambridge Univ. Press, 2012).
- 531 Kato, K.: On the Abrupt Change in the Structure of the Baiu Front over the China
532 Continent in Late May of 1979. *Journal of the Meteorological Society of Japan*,
533 63(1), 20-36, https://doi:10.2151/jmsj1965.63.1_20, 1985.
- 534 Kazuki, T., Oliver C. S. V., Masahiro, R.: Spatial variability of precipitation and soil
535 moisture on the 2011 flood at chao phraya river basin. *International Water*
536 *Technology Association, Proceedings of Hydrology and Water Resources*, B, 17-
537 21, 2013.
- 538 Kemter, M., Merz, B., Marwan, N., Vorogushyn, S., & Blöschl, G.: Joint trends in flood
539 magnitudes and spatial extents across Europe. *Geophysical Research Letters*, 47,
540 e2020GL087464. <https://doi.org/10.1029/2020GL087464>, 2020.
- 541 Lehner, B., C. Reidy Liermann, C. Revenga, C. Vörösmarty, B. Fekete, P. Crouzet, P.
542 Döll, M. Endejan, K. Frenken, J. Magome, C. Nilsson, J.C. Robertson, R. Rodel,
543 N. Sindorf, and D. Wisser. 2011. High-resolution mapping of the world's
544 reservoirs and dams for sustainable river-flow management. *Frontiers in Ecology*
545 *and the Environment* 9 (9): 494-502.
- 546 Li, Q., Wei, F. and Li, D.: Interdecadal variation of East Asian summer monsoon and
547 drought/flood distribution over eastern China in the last 159 years. *Journal of*
548 *Geographical Sciences*, 21(4), 579-593, <https://doi:10.1007/s11442-011-0865-2>,
549 2011.
- 550 Li, X., Zhang, K., Gu, P., Feng, H., Yin, Y., Chen, W. and Cheng, B.: Changes in
551 precipitation extremes in the Yangtze River Basin during 1960-2019 and the
552 association with global warming, ENSO, and local effects. *Science of the Total*
553 *Environment*, 760, <https://doi:10.1016/j.scitotenv.2020.144244>, 2021.



-
- 554 Liu, B., Yan, Y., Zhu, C., Ma, S., & Li, J.: Record-breaking Meiyu rainfall around the
555 Yangtze River in 2020 regulated by the subseasonal phase transition of the North
556 Atlantic Oscillation. *Geophysical Research Letters*, 47, e2020GL090342.
557 <https://doi.org/10.1029/2020GL090342>, 2020.
- 558 Liu, L., Ye, S., Chen, C., Pan, H. and Ran, Q.: Nonsequential Response in Mountainous
559 Areas of Southwest China. *Frontiers in Earth Science*, 9: 1-15. doi:
560 10.3389/feart.2021.660244, 2021
- 561 Liu, N., Jin, Y. and Dai, J.: Variation of Temperature and Precipitation in Urban
562 Agglomeration and Prevention Suggestion of Waterlogging in Middle and Lower
563 Reaches of Yangtze River. 3rd International Conference on Energy Equipment
564 Science and Engineering (Iceese 2017), 128, <https://doi.org/10.1088/1755-1315/128/1/012165>, 2018.
- 566 Liu, S., Huang, S., Xie, Y., Wang, H., Leng, G., Huang, Q., Wei, X., and Wang, L.:
567 Identification of the Non-stationarity of Floods: Changing Patterns, Causes, and
568 Implications, *Water Resour. Manag.*, 33, 939–953, 2018.
- 569 Liu, Y., Xinyu, L., Liancheng, Z., Yang, L., Chunrong, J., Ni, W. and Juan, Z.:
570 Quantifying rain, snow and glacier meltwater in river discharge during flood
571 events in the Manas River Basin, China. *Natural Hazards*, 108(1), 1137-1158,
572 <https://doi.org/10.1007/s11069-021-04723-8>, 2021.
- 573 Long, L.H., Ji, D.B., Yang, Z.Y., Cheng, H.Q., Yang, Z.J., Liu, D.F., Liu, L. and Lorke,
574 A.: Tributary oscillations generated by diurnal discharge regulation in Three
575 Gorges Reservoir. *Environmental Research Letters*, 15(8),
576 <https://doi.org/10.1088/1748-9326/ab8d80>, 2020.
- 577 Lu, M., Wu, S.-J., Chen, J., Chen, C., Wen, Z. and Huang, Y.: Changes in extreme
578 precipitation in the Yangtze River basin and its association with global mean
579 temperature and ENSO. *International Journal of Climatology*, 38(4), 1989-2005,
580 <https://doi.org/10.1002/joc.5311>, 2018.
- 581 Miao, Q., Huang, M. and Li, R., Q.: Response of net primary productivity of vegetation
582 in Yangtze River Basin to future climate change. *Journal of Natural Resources*, 25,
583 08(2010):1296-1305, doi:CNKI:SUN:ZRZX.0.2010-08-007, 2015.
- 584 Munoz, S.E., Giosan, L., Therrell, M.D., Remo, J.W.F., Shen, Z., Sullivan, R.M.,
585 Wiman, C., O'Donnell, M., and Donnelly, J.P.: Climatic control of Mississippi
586 River flood hazard amplified by river engineering, 556, 95 – 98, 2018.



-
- 587 Musselman, K.N., Lehner, F., Ikeda, K., Clark, M.P., Prein, A.F., Liu, C., Barlage, M.
588 and Rasmussen, R.: Projected increases and shifts in rain-on-snow flood risk over
589 western North America, *Nature Climate Change*, 8, 808 – 812, 2018.
- 590 Ohmura, A. and Wild, M.: Is the hydrological cycle accelerating? *Science*, 298, 1345–
591 1346, 2002.
- 592 Pegram, G. and Bardossy, A.: Downscaling Regional Circulation Model rainfall to
593 gauge sites using recorrelation and circulation pattern dependent quantile-quantile
594 transforms for quantifying climate change. *Journal of Hydrology*, 504, 142-159,
595 <https://doi.org/10.1016/j.jhydrol.2013.09.014>, 2013.
- 596 Peng, T., Tian, H., Singh, V. P., Chen, M., Liu, J., Ma, H. B. and Wang, J. B.:
597 Quantitative assessment of drivers of sediment load reduction in the Yangtze River
598 basin, China, *Journal of Hydrology*, 580,
599 <https://doi.org/10.1016/j.jhydrol.2019.124242>, 2020.
- 600 Qian, H. and Xu, S.-B.: Prediction of Autumn Precipitation over the Middle and Lower
601 Reaches of the Yangtze River Basin Based on Climate Indices. *Climate*, 8(4),
602 <https://doi.org/10.3390/cli8040053>, 2020.
- 603 Ran, Q., Zong, X., Ye, S., Gao, J. and Hong, Y.: Dominant mechanism for annual
604 maximum flood and sediment events generation in the Yellow River basin. *Catena*,
605 187, <https://doi.org/10.1016/j.catena.2019.104376>, 2020.
- 606 Ray S. M., Ramakar J. and Kishanjit K. K.: Precipitation-runoff simulation for a
607 Himalayan River Basin, India using artificial neural network algorithms, *Sciences
608 in Cold and Arid Regions*, 5(1), 85-95, 2013.
- 609 Rottler, E., Francke, T., Burger, G., and Bronstert, A.: Long-term changes in central
610 European river discharge for 1869–2016: impact of changing snow covers,
611 reservoir constructions and an intensified hydrological cycle, *Hydrol. Earth Syst.
612 Sci.*, 24, 1721–1740, 2020.
- 613 Sharma, A., Wasko, C. and Lettenmaier, D.P.: If Precipitation Extremes Are Increasing,
614 Why Aren't Floods? *Water Resources Research*, 54(11), 8545-8551,
615 <https://doi.org/10.1029/2018WR023749>, 2018.
- 616 Smith, J. A., Cox, A. A., Baeck, M. L., Yang, L., and Bates, P.: Strange floods: the
617 upper tail of flood peaks in the United States, *Water Resour. Res.*, 54, 6510–6542,
618 2018.



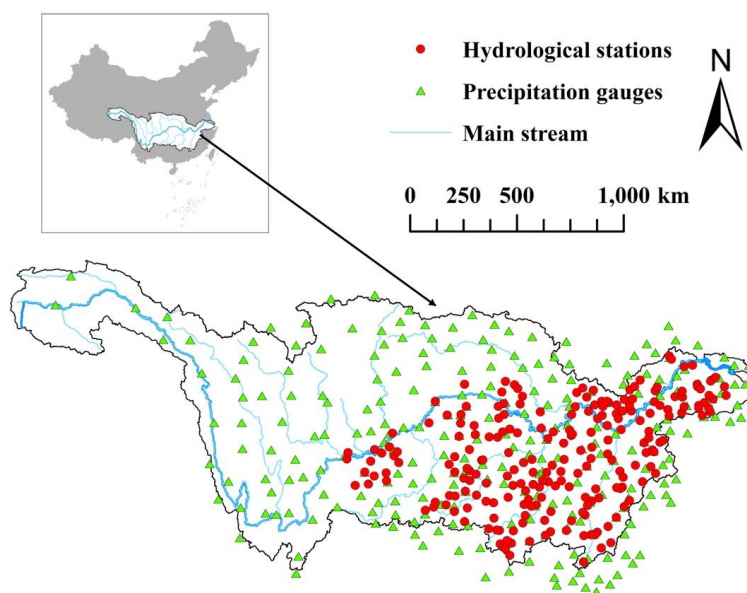
-
- 619 Su, Z., Ho, M., Hao, Z., Lall, U., Sun, X., Chen, X. and Yan, L.: The impact of the
620 Three Gorges Dam on summer streamflow in the Yangtze River Basin.
621 Hydrological Processes, 34(3), 705-717, [https://doi:10.1002/hyp.13619](https://doi.org/10.1002/hyp.13619), 2020.
- 622 Suresh, S. S., Benefit O., Augustine T., and Trevor P.: Peoples' Perception on the
623 Effects of Floods in the Riverine Areas of Ogbia Local Government Area of
624 Bayelsa State, Nigeria, Knowledge Management, [https://doi:10.18848/2327-7998/CGP/v12i02/50793](https://doi.org/10.18848/2327-7998/CGP/v12i02/50793), 2013.
- 626 Tao, S. Y., Rainstorm in China [M], Beijing: Science Press, 1980.(in Chinese)
- 627 Trambly, Y., Villarini, G., El Khalki, E. M., Gründemann, G., & Hughes, D.:
628 Evaluation of the drivers responsible for flooding in Africa. Water Resources
629 Research, 57, e2021WR029595. <https://doi.org/10.1029/2021WR029595>, 2021.
- 630 Vicente-Serrano, S.M., Azorin-Molina, C., Sanchez-Lorenzo, A., Revuelto, J., Lopez-
631 Moreno, J.I., Gonzalez-Hidalgo, J.C., Moran-Tejeda, E. and Espejo, F.: Reference
632 evapotranspiration variability and trends in Spain, 1961-2011. Global and
633 Planetary Change, 121, 26-40, [https://doi:10.1016/j.gloplacha.2014.06.005](https://doi.org/10.1016/j.gloplacha.2014.06.005), 2014.
- 634 Volpi, E., Di Lazzaro, M., Bertola, M., Viglione, A. and Fiori, A.: Reservoir Effects on
635 Flood Peak Discharge at the Catchment Scale. Water Resources Research, 54(11),
636 9623-9636, [https://doi:10.1029/2018wr023866](https://doi.org/10.1029/2018wr023866), 2018.
- 637 Wang, H., Zhou, Y., Pang, Y. and Wang, X.: Fluctuation of Cadmium Load on a Tide-
638 Influenced Waterfront Lake in the Middle-Lower Reaches of the Yangtze River.
639 Clean-Soil Air Water, 42(10), 1402-1408, [https://doi:10.1002/clen.201300693](https://doi.org/10.1002/clen.201300693),
640 2014.
- 641 Wang, J., Ran, Q., Liu, L., Pan, H. and Ye, S.: Study on the Dominant Mechanism of
642 Extreme Flow Events in the Middle and Lower Reaches of the Yangtze River,
643 China Rural Water and Hydropower, Accepted.
- 644 Wang, R., Yao, Z., Liu, Z., Wu, S., Jiang, L. and Wang, L.: Snow cover variability and
645 snowmelt in a high-altitude ungauged catchment. Hydrological Processes, 29(17),
646 3665-3676, [https://doi:10.1002/hyp.10472](https://doi.org/10.1002/hyp.10472), 2015.
- 647 Wang, W., Xing W., Yang, T., Shao, Q., Peng, S., Yu, Z., and Yong, B.: Characterizing
648 the changing behaviours of precipitation concentration in the Yangtze River Basin,
649 China. Hydrological Processes, 27(24), 3375-3393, [https://doi: 10.1002/hyp.9430](https://doi.org/10.1002/hyp.9430),
650 2013.



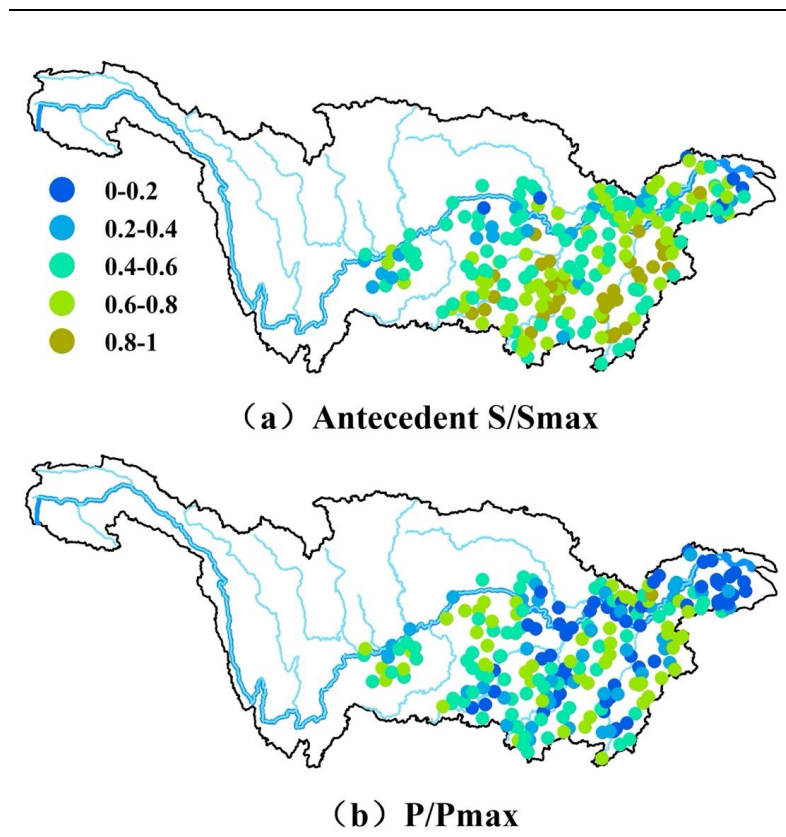
-
- 651 Wang, Z. and Plate, E.: Recent flood disasters in China. Proceedings of the Institution
652 of Civil Engineers – Water and Maritime Engineering (3),
653 <https://doi:10.1680/wame.2002.154.3.177>, 2002.
- 654 Wasko, C. and Nathan, R.: Influence of changes in rainfall and soil moisture on trends
655 in flooding. Journal of Hydrology, 575, 432-441,
656 <https://doi:10.1016/j.jhydrol.2019.05.054>, 2019.
- 657 Wasko, C., Nathan, R., & Peel, M. C.: Changes in antecedent soil moisture modulate
658 flood seasonality in a changing climate. Water Resources Research, 56,
659 e2019WR026300. <https://doi.org/10.1029/2019WR026300>, 2020.
- 660 Wu, X. S., Guo, S. L. and Ba, H. H.: Long-term precipitation forecast method based on
661 SST multipole index, Journal of water conservancy(10), 1276-1283,
662 <https://doi:10.13243/j.cnki.slx.20180544>, 2018.
- 663 Xia, J. and Chen, J.: A new era of flood control strategies from the perspective of
664 managing the 2020 Yangtze River flood. Science China-Earth Sciences, 64(1), 1-
665 9, <https://doi:10.1007/s11430-020-9699-8>, 2021.
- 666 Xie, Z., Du, Y., Zeng, Y. and Miao, Q.: Classification of yearly extreme precipitation
667 events and associated flood risk in the Yangtze-Huaihe River Valley. Science
668 China-Earth Sciences, 61(9), 1341-1356, <https://doi:10.1007/s11430-017-9212-8>,
669 2018.
- 670 Yang, H.F., Yang, S.L., Xu, K.H., Milliman, J.D., Wang, H., Yang, Z., Chen, Z. and
671 Zhang, C.Y.: Human impacts on sediment in the Yangtze River: A review and new
672 perspectives. Global and Planetary Change, 162, 8-17,
673 <https://doi:10.1016/j.gloplacha.2018.01.001>, 2018.
- 674 Yang, L., Wang, L., Li, X. and Gao, J.: On the flood peak distributions over China.
675 Hydrology and Earth System Sciences, 23(12), 5133-5149,
676 <https://doi:10.5194/hess-23-5133-2019>, 2019.
- 677 Yang, W., Yang, H., and Yang, D.: Classifying floods by quantifying driver
678 contributions in the Eastern Monsoon Region of China, Journal of Hydrology, 585,
679 124767, 2020.
- 680 Yang, W., Yang, H., Yang, D., and Hou, A.: Causal effects of dams and land cover
681 changes on flood changes in mainland China. Hydrol. Earth Syst. Sci., 25, 2705–
682 2720, 2021.



-
- 683 Ye, S., Li, H., Leung, L.R., Guo, J., Ran, Q., Demissie, Y., et al., 2017. Understanding
684 flood seasonality and its temporal shifts within the contiguous United States. *J.*
685 *Hydrometeorol.* 18 (7), 1997–2009.
- 686 Ye, X., Xu, C.-Y., Li, Y., Li, X. and Zhang, Q.: Change of annual extreme water levels
687 and correlation with river discharges in the middle-lower Yangtze River:
688 Characteristics and possible affecting factors. *Chinese Geographical*
689 *Science*,27(2), 325-336, <https://doi:10.1007/s11769-017-0866-x>, 2017.
- 690 Yu, F., Chen, Z., Ren, X. and Yang, G.: Analysis of historical floods on the Yangtze
691 River, China: Characteristics and explanations. *Geomorphology*,113(3-4), 210-
692 216, <https://doi:10.1016/j.geomorph.2009.03.008>, 2009.
- 693 Zhang, H., Liu, S., Ye, J. and Yeh, P.J.F.: Model simulations of potential contribution
694 of the proposed Huangpu Gate to flood control in the Lake Taihu basin of China.
695 *Hydrology and Earth System Sciences*, 21(10), 5339-5355,
696 <https://doi:10.5194/hess-21-5339-2017>, 2017.
- 697 Zhao, J., Li, J., Yan, H., Zheng, L. and Dai, Z.: Analysis on the Water Exchange
698 between the Main Stream of the Yangtze River and the Poyang Lake. 2011 3rd
699 International Conference on Environmental Science and Information Application
700 Technology Esiat 2011, Vol 10, Pt C,10, 2256-2264,
701 <https://doi:10.1016/j.proenv.2011.09.353>, 2011.
- 702 Zhang, S., Kang, L. and He, X.: Equal proportion flood retention strategy for the leading
703 multireservoir system in upper Yangtze River. *International Conference on Water*
704 *Resources and Environment, WRE 2015*, 2015.
- 705 Zhang, W., Villarini, G., Vecchi, G.A. and Smith, J. A.: Urbanization exacerbated the
706 rainfall and flooding caused by hurricane Harvey in Houston. *Nature*, 563, 384 –
707 388, 2018.
- 708 Zou, B., Li, Y., Feng, B.: Analysis on dispatching influence of Three Gorges Reservoir
709 on water level of main stream in mid-lower reaches of Yangtze River: a case study
710 of flood in July,2010. *Yangtze River*, 42.06:80-82+100. doi:10.16232/j.cnki.1001-
711 4179.2011.06.004, 2011.
- 712
713



714
715 **Figure 1:** Map of the Yangtze River basin, and the climate stations and hydrological
716 stations. The blue line is the main stream of Yangtze River.
717



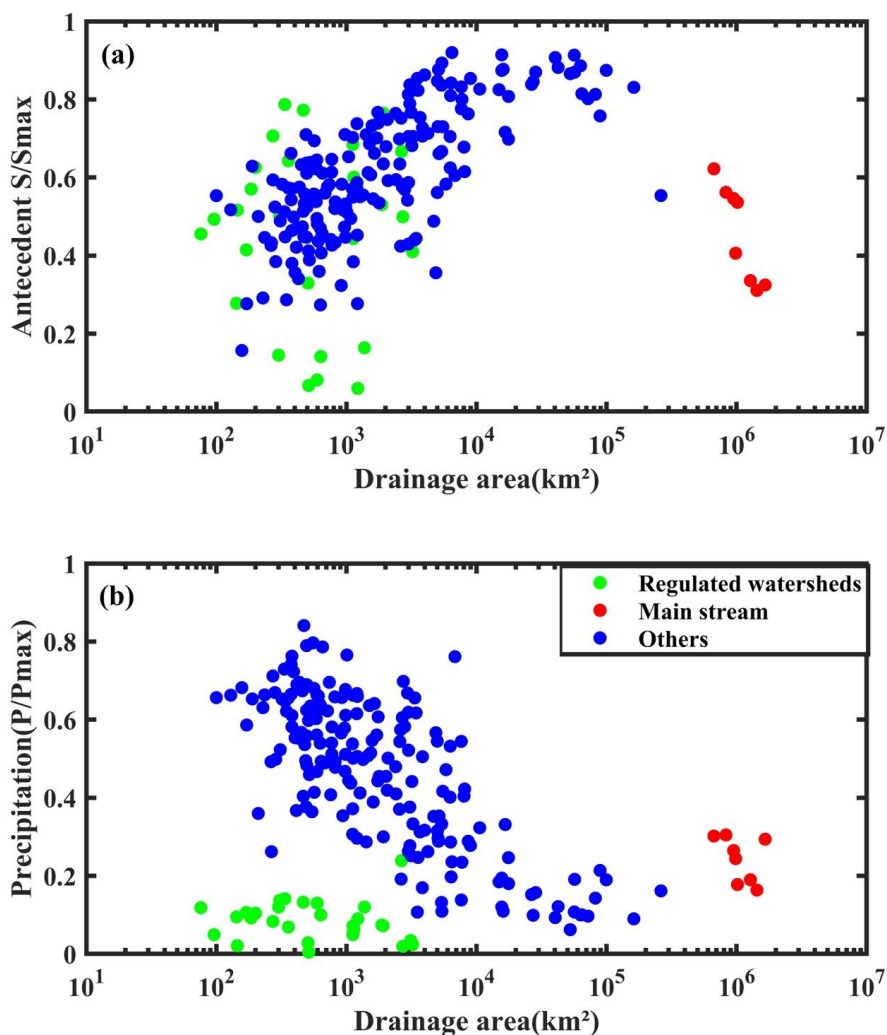
718

719 **Figure 2:** the spatial distribution of (a) antecedent soil moisture during annual

720 maximum flood, normalized by maximum storage; (b) daily precipitation during annual

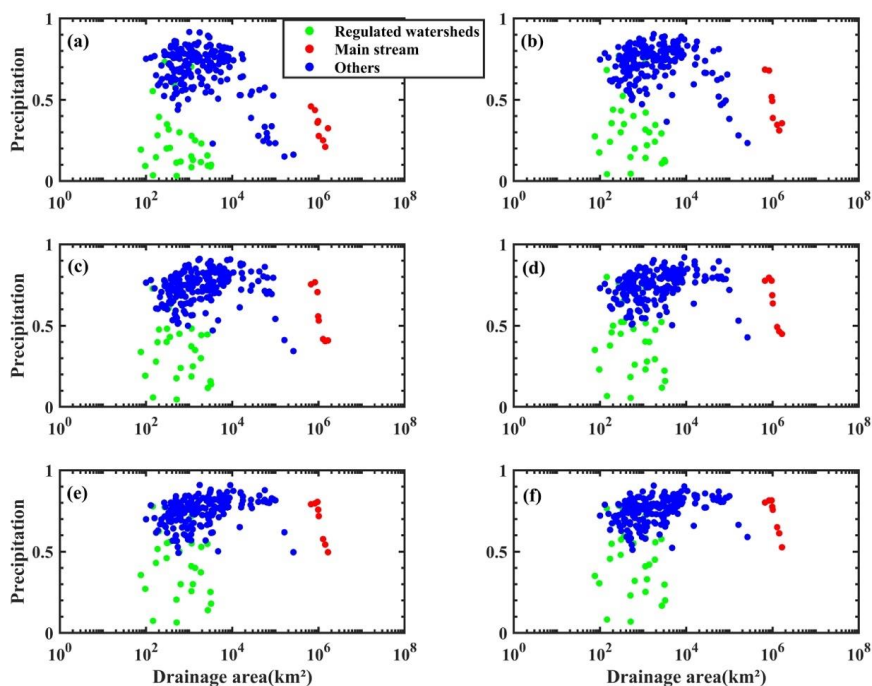
721 maximum flood, normalized by maximum daily precipitation.

722

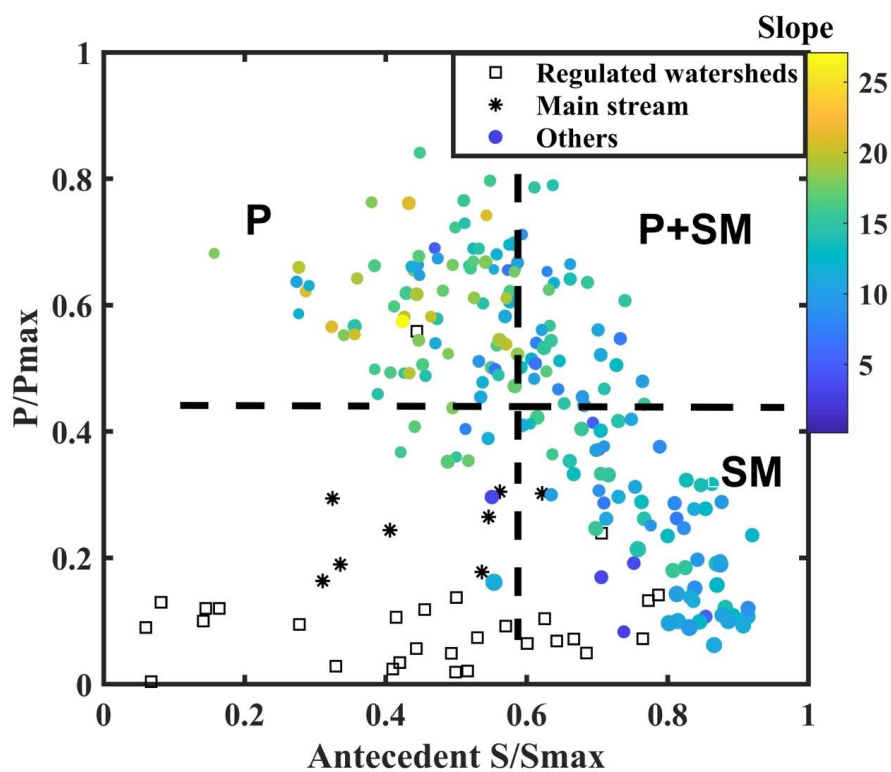


723
724 **Figure 3:** Scatterplot between the drainage area and (a) the antecedent soil moisture of
725 AMF events normalized by maximum storage (the linear regression for blue dots: $R^2 =$
726 0.46 , p -value <0.001); (b) the precipitation at the day of AMF events normalized by
727 maximum daily precipitation (the linear regression for blue dots: $R^2 = 0.61$, p -
728 value <0.001). The green ones represent the regulated watershed, the red ones represent
729 the sites on the main stream, and the rest sites are shown in blue.

730
731
732



733
734 **Figure 4:** Scatterplot between the drainage area and the accumulated rainfall of (a) two
735 days; (b) three days; (c) four days; (d) five days; (e) six days; and (f) seven days on
736 AMF events, normalized by maximum of accumulated precipitation.
737

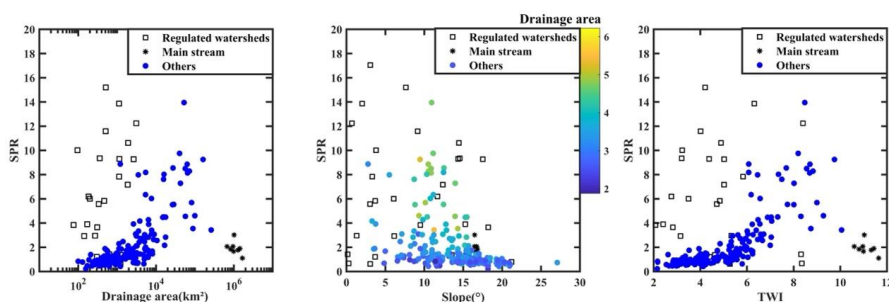


738

739 **Figure 5:** Scatterplot of the normalized rainfall and antecedent soil moisture, the color
740 represents topographic gradient and the size of circles is scaled by drainage area.

741

742



743

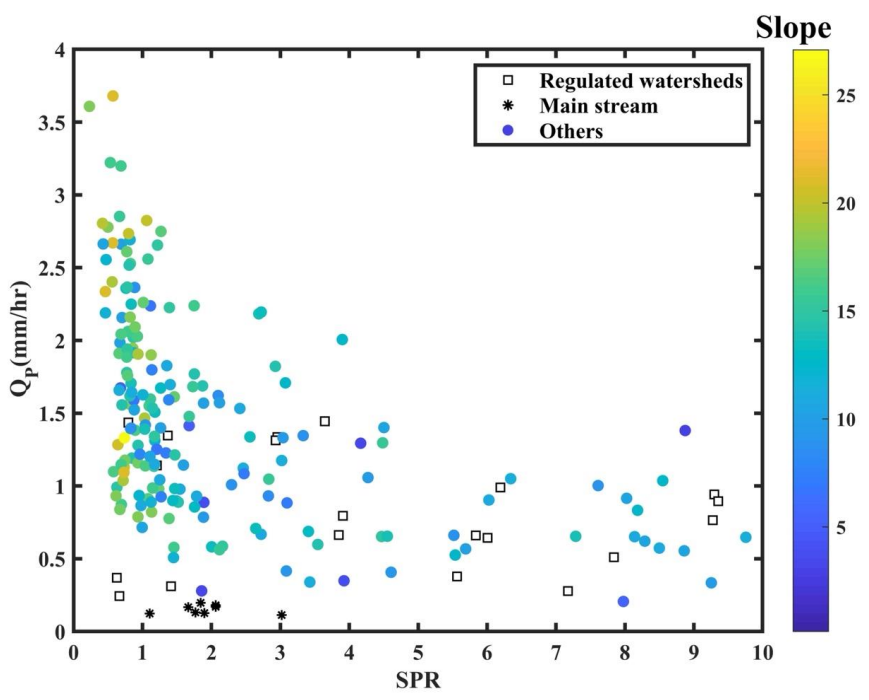
744

745

746

747

Figure 6: Scatterplots between the ratio of antecedent soil saturation rate and normalized precipitation (SPR) and (a) drainage area; (b) slope; and (c) topographic wetness index (TWI).



748

749 **Figure 7:** Scatterplot between the ratio of antecedent soil saturation rate and normalized
750 precipitation (SPR) and area weighted annual maximum discharge (Q_p), the color
751 represents topographic gradient.